

Lecture 08

Fixed Wing UAV Dynamics and Control

Professor Hugh H.T. Liu (UTIAS)

November 4, 2021

AER1216 - Fundamentals of UAS

FW UAV Dyn & Ctrl

H.H.T. Liu © 2021

Outline

- 1 Aircraft Reference Frames
- 2 Equations of Motion in Body-Fixed Frame
- 3 Linearized Dynamics
- 4 Flight Control Surfaces
- 5 Mission Profile
- 6 Control Design Process
- 7 Feedback Control Theory
- 8 Pitch Attitude Control
- 9 Autopilot: Altitude Hold Control
- 10 Procerus Flying Wing System



Fixed Wing UAV vs Multi-Rotor UAV

- aerodynamic effects
- diversified control effectors

leading to distinctive performance characteristics and dynamic behaviour



1. Aircraft Reference Frames

An Earth-surface fixed frame $\mathcal{F}_E : \{O_E, \underline{x}_E, \underline{y}_E, \underline{z}_E\}$ is often treated as an inertial frame, with its origin on a fixed Earth surface location; axis \underline{z}_E directed vertically down; \underline{x}_E points north, and \underline{y}_E east. Sometimes it is also called the NED frame.



The body-fixed reference frame $\mathcal{F}_B : \{O_{cm}, \underline{x}_B, \underline{y}_B, \underline{z}_B\}$ is fixed to the vehicle (therefore, the angular velocity of the frame is the same as that of the body), the origin is usually chosen at the centre of mass, the axes $\underline{x}_B, \underline{z}_B$ are chosen in the plane of vertical symmetry, \underline{x}_B points towards the nose of aircraft, \underline{y}_B to the right-wing tip, and \underline{z} is directed downwards perpendicular to the vertical plane.

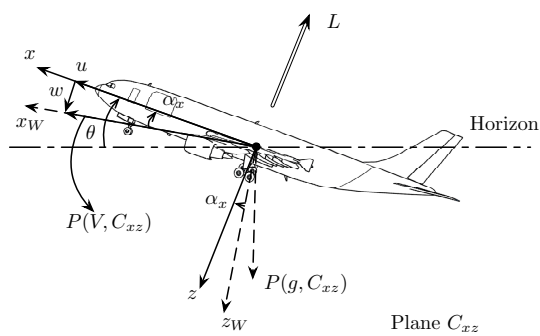


Fig 1: Body-Fixed Frame



The air-trajectory reference frame is also called the *wind frame*: $\mathcal{F}_W : \{O_{cm}, \underline{x}_W, \underline{y}_W, \underline{z}_W\}$. It has origin fixed to the vehicle (usually at the centre of mass), and \underline{x}_W is directed along the velocity vector \underline{v} of the vehicle relative to the atmosphere. The axis \underline{z}_W maintains in the plane of symmetry of the vehicle. If the atmosphere is at rest, then O_{cm} would trace out the trajectory of the vehicle relative to the Earth, and \underline{x}_W would be always tangent to it. [?]

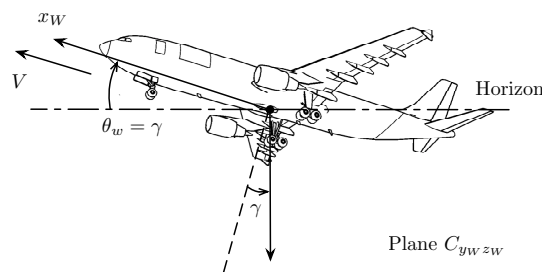


Fig 2: Air-Trajectory Frame or Wind Axes



The rotation matrix from \mathcal{F}_E to \mathcal{F}_B is given by

$$\underline{\mathbf{F}}_B = \underline{\mathbf{C}}_{BE} \underline{\mathbf{F}}_E \quad (1)$$

where $\underline{\mathbf{C}}_{BE} = \underline{\mathbf{C}}_1(\phi) \underline{\mathbf{C}}_2(\theta) \underline{\mathbf{C}}_3(\psi) =$

$$\begin{bmatrix} \cos \theta \cos \psi & \cos \theta \sin \psi & -\sin \theta \\ \sin \phi \sin \theta \cos \psi - \cos \phi \sin \psi & \sin \phi \sin \theta \sin \psi + \cos \phi \cos \psi & \sin \phi \cos \theta \\ \cos \phi \sin \theta \cos \psi + \sin \phi \sin \psi & \cos \phi \sin \theta \sin \psi - \sin \phi \cos \psi & \cos \phi \cos \theta \end{bmatrix} \quad (2)$$



Aircraft Velocity Expressions

Aircraft velocity vector $\underline{\mathbf{v}}$ may have different numerical vectorial expressions under different reference frames:

$$\underline{\mathbf{v}}_E = \begin{bmatrix} \dot{x}_E \\ \dot{y}_E \\ \dot{z}_E \end{bmatrix} = \underline{\mathbf{C}}_{EB} \underline{\mathbf{v}}_B = \underline{\mathbf{C}}_{EB} \begin{bmatrix} u \\ v \\ w \end{bmatrix} \quad (3)$$

$$\underline{\mathbf{v}}_E = \begin{bmatrix} \dot{x}_E \\ \dot{y}_E \\ \dot{z}_E \end{bmatrix} = \underline{\mathbf{C}}_{EW} \begin{bmatrix} V \\ 0 \\ 0 \end{bmatrix} = \begin{bmatrix} V \cos \gamma \cos \sigma \\ V \cos \gamma \sin \sigma \\ -V \sin \gamma \end{bmatrix} \quad (4)$$

$$\underline{\mathbf{v}}_B = \begin{bmatrix} u \\ v \\ w \end{bmatrix} = \underline{\mathbf{C}}_{BW} \begin{bmatrix} V \\ 0 \\ 0 \end{bmatrix} = \begin{bmatrix} V \cos \alpha \cos \beta \\ V \sin \beta \\ V \sin \alpha \cos \beta \end{bmatrix} \quad (5)$$



The angular velocity of \mathcal{F}_B relative to \mathcal{F}_E is denoted by $\vec{\omega}$. Its numerical expression is given as follows:

$$\vec{\omega} = \underline{F}_B^T \underline{\omega}_B$$

where

$$\underline{\omega}_B = \begin{bmatrix} p \\ q \\ r \end{bmatrix}$$

$$\begin{bmatrix} p \\ q \\ r \end{bmatrix} = \begin{bmatrix} 1 & 0 & -\sin \theta \\ 0 & \cos \phi & \sin \phi \cos \theta \\ 0 & -\sin \phi & \cos \phi \cos \theta \end{bmatrix} \begin{bmatrix} \dot{\phi} \\ \dot{\theta} \\ \dot{\psi} \end{bmatrix} \triangleq \underline{S}_B \begin{bmatrix} \dot{\phi} \\ \dot{\theta} \\ \dot{\psi} \end{bmatrix} \quad (6)$$



10

Aircraft Kinematics Block Diagram

After all, the aircraft kinematics can be represented by the following figure.

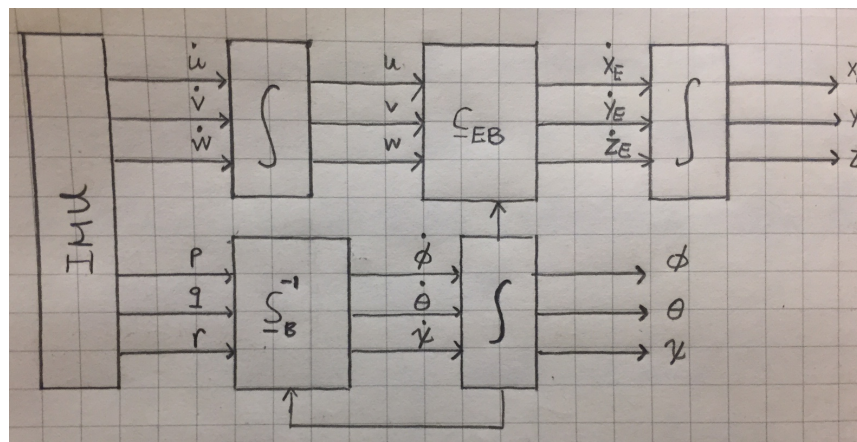


Fig 3: Vehicle Kinematics Diagram



11

2. Equations of Motion in Body-Fixed Frame

Given the expressions under body-fixed frame $\mathcal{F}_B : \{\underline{x}, \underline{y}, \underline{z}\}$:

$$\underline{f}_B = [X \ Y \ Z]^T \quad (7)$$

$$\underline{\omega}_B = [p \ q \ r]^T \quad (8)$$

$$\underline{v}_B = [u \ v \ w]^T \quad (9)$$



12

one gets the following force equation expressions:

$$\underline{f}_B = m(\dot{\underline{v}}_B + \underline{\omega}_B^{\times} \underline{v}_B) \quad (10)$$

leading to

$$X = m(\dot{u} + qw - rv) \quad (11)$$

$$Y = m(\dot{v} + ru - pw) \quad (12)$$

$$Z = m(\dot{w} + pv - qu) \quad (13)$$



13

Given the expressions in Body-Fixed Frame \mathcal{F}_B :

$$\underline{\tau}_B^{cm} = [L \ M \ N]^T \quad (14)$$

$$\underline{I}_B = \begin{bmatrix} I_{xx} & I_{xy} & I_{xz} \\ I_{yx} & I_{yy} & I_{yz} \\ I_{zx} & I_{zy} & I_{zz} \end{bmatrix} \quad (15)$$

According to

$$\underline{\tau}_B = \underline{\omega}_B^{\times} \underline{I}_B \underline{\omega}_B + \underline{I}_B \underline{\omega}_B \cdot \underline{j}_B \quad (16)$$

$$\begin{aligned} L &= I_{xx}\dot{p} + I_{xy}(\dot{q} - pr) + I_{xz}(\dot{r} + pq) + I_{yz}(q^2 - r^2) - (I_{yy} - I_{zz})qr \\ M &= I_{yy}\dot{q} + I_{yz}(\dot{r} - pq) + I_{yx}(\dot{p} + qr) + I_{zx}(r^2 - p^2) - (I_{zz} - I_{xx})pr \\ N &= I_{zz}\dot{r} + I_{zx}(\dot{p} - qr) + I_{zy}(\dot{q} + pr) + I_{xy}(p^2 - q^2) - (I_{xx} - I_{yy})pq \end{aligned}$$



14

Given the aircraft forces (propulsion \underline{T} , aerodynamic lift \underline{L} , drag \underline{D} , side force \underline{Y} , and gravity \underline{W}) expressed in a mixed frame axes, as

$$\underline{f} = W\underline{z}_E + T\underline{x}_B - D\underline{x}_W - L\underline{z}_W - Y\underline{y}_W \quad (17)$$

where \underline{z}_E is the \underline{z} axis of the Earth-surface frame \mathcal{F}_E , \underline{x}_B is the \underline{x} axis of the body-fixed frame \mathcal{F}_B , $\underline{x}_W, \underline{y}_W, \underline{z}_W$ are the axes of the air-trajectory frame \mathcal{F}_W , respectively.



15

$$\underline{f}_B = \begin{bmatrix} T - Ws_\theta - Dc_\alpha c_\beta + Yc_\alpha s_\beta + Ls_\alpha \\ Ws_\phi c_\theta - Ds_\beta - Yc_\beta \\ Wc_\phi c_\theta - Ds_\alpha c_\beta + Ys_\alpha s_\beta - Lc_\alpha \end{bmatrix} \approx \begin{bmatrix} T - Ws_\theta - D \\ Ws_\phi c_\theta - Y \\ Wc_\phi c_\theta - L \end{bmatrix} \quad (18)$$



16

Dynamics Diagram

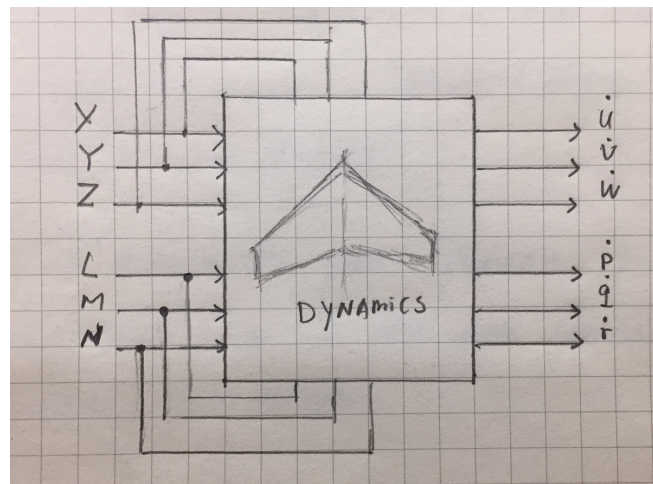


Fig 4: Aerial Vehicle Dynamics Diagram



17

3. Linearized Dynamics

- approximation of aerodynamic forces and moments
- separation of longitudinal and lateral motions
- small disturbance theory about an equilibrium point (steady flight state)
- specialized simplifications or further approximations for specific configuration



18

The aerodynamic forces and moments, as we know by now, are also functions of flight motion variables, i.e., speed u, v, w components, angular rate p, q, r and their rates. We can represent

$$\Delta F_{aero} = F(u, v, w, p, q, r, \dot{u}, \dot{v}, \dot{w}, \dot{p}, \dot{q}, \dot{r}) \quad (19)$$

Thus the aerodynamic force is approximated by its series expansion of the right-hand side of this equation, based on an equilibrium point (in subscript e):

$$\Delta F_{aero} = F_e + F_u u + F_v v + F_w w + F_{\dot{u}} \dot{u} + F_{\dot{v}} \dot{v} + F_{\dot{w}} \dot{w} + F_p p + F_q q + F_r r + F_{\dot{p}} \dot{p} + F_{\dot{q}} \dot{q} + F_{\dot{r}} \dot{r} \quad (20)$$

where each term has a partial derivative picks up its value at the same equilibrium point:

$$F_u = \left(\frac{\partial F}{\partial u} \right)_e \quad (21)$$

and so on. They are known as the *stability derivatives*, or more generally as *aerodynamic derivatives*.



Further, we adopt another approximation, that is, the separation of longitudinal (of vertical symmetric plane) motions from lateral (out of vertical symmetric plane) motions, and corresponding separation of longitudinal forces/moment (forces acting on the x- and z-axes as well as the pitching moment about y-axis) from lateral forces/moment (y- side force, as well as rolling, yawing moments). It states that longitudinal motions dominate the impact on the longitudinal forces and moments, vice versa. Then we have separate derivatives, as follows:

$$\begin{bmatrix} X_u & X_w & X_q & X_{\dot{u}} & X_{\dot{w}} & X_{\dot{q}} \\ Z_u & Z_w & Z_q & Z_{\dot{u}} & Z_{\dot{w}} & Z_{\dot{q}} \\ M_u & M_w & M_q & M_{\dot{u}} & M_{\dot{w}} & M_{\dot{q}} \end{bmatrix} \begin{bmatrix} Y_v & Y_p & Y_r & Y_{\dot{v}} & Y_{\dot{p}} & Y_{\dot{r}} \\ L_v & L_p & L_r & L_{\dot{v}} & L_{\dot{p}} & L_{\dot{r}} \\ N_v & N_p & N_r & N_{\dot{v}} & N_{\dot{p}} & N_{\dot{r}} \end{bmatrix} \quad (22)$$



20

Thus one has

$$\begin{bmatrix} \Delta X \\ \Delta Z \\ \Delta M \end{bmatrix} = \begin{bmatrix} X_u & X_w & X_q & X_{\dot{u}} & X_{\dot{w}} & X_{\dot{q}} \\ Z_u & Z_w & Z_q & Z_{\dot{u}} & Z_{\dot{w}} & Z_{\dot{q}} \\ M_u & M_w & M_q & M_{\dot{u}} & M_{\dot{w}} & M_{\dot{q}} \end{bmatrix} \cdot \begin{bmatrix} u \\ w \\ q \\ \dot{u} \\ \dot{w} \\ \dot{q} \end{bmatrix} + \begin{bmatrix} \Delta X_c \\ \Delta Z_c \\ \Delta M_c \end{bmatrix}$$

$$\begin{bmatrix} \Delta Y \\ \Delta L \\ \Delta N \end{bmatrix} = \begin{bmatrix} Y_v & Y_p & Y_r & Y_{\dot{v}} & Y_{\dot{p}} & Y_{\dot{r}} \\ L_v & L_p & L_r & L_{\dot{v}} & L_{\dot{p}} & L_{\dot{r}} \\ N_v & N_p & N_r & N_{\dot{v}} & N_{\dot{p}} & N_{\dot{r}} \end{bmatrix} \cdot \begin{bmatrix} v \\ r \\ p \\ \dot{v} \\ \dot{r} \\ \dot{p} \end{bmatrix} + \begin{bmatrix} \Delta Y_c \\ \Delta L_c \\ \Delta N_c \end{bmatrix}$$



21

Steady States

A typical equilibrium operating condition for aircraft would be that the aircraft is flying in a steady, symmetric flight (e.g. level flight, $\gamma = 0$, constant speed $V = U_e$).

$$\begin{cases} X_e - W \sin \theta_e = 0 \\ Z_e + W \cos \theta_e = 0 \\ M_e = 0 \end{cases} \quad (23)$$

$$\begin{cases} Y_e = 0 \\ L_e = 0 \\ N_e = 0 \end{cases} \quad (24)$$



22

Longitudinal Equation

Assume the reference flight condition to be symmetric, unaccelerated, steady, and with no angular velocity, therefore

$$\begin{aligned} X_e - mg \sin \theta_e &= 0 & Y_e &= 0 & Z_e + mg \cos \theta_e &= 0 \\ L_e &= 0 & M_e &= 0 & N_e &= 0 \\ P_e &= 0 & Q_e &= 0 & R_e &= 0 \\ U_e &= U_e & V_e &= 0 & W_e &= 0 \\ \theta_e & \psi_e = 0 & \phi_e &= 0 \end{aligned}$$



23

Assuming small disturbance

$$\begin{aligned}
 X &= X_e + \underbrace{\Delta X}_x & Y &= \underbrace{Y_e}_0 + \underbrace{\Delta Y}_y & Z &= Z_e + \underbrace{\Delta Z}_z \\
 L &= \underbrace{L_e}_0 + \Delta L & M &= \underbrace{M_e}_0 + \Delta M & N &= \underbrace{N_e}_0 + \Delta N \\
 P &= \underbrace{P_e}_0 + \underbrace{\Delta P}_p & Q &= \underbrace{Q_e}_0 + \underbrace{\Delta Q}_q & R &= \underbrace{R_e}_0 + \underbrace{\Delta R}_r \\
 U &= U_e + \underbrace{\Delta U}_u & V &= \underbrace{V_e}_0 + \underbrace{\Delta V}_v & W &= \underbrace{W_e}_0 + \underbrace{\Delta W}_w \\
 \theta &= \theta_e + \Delta\theta & \psi &= \underbrace{\psi_e}_0 + \Delta\psi & \phi &= \underbrace{\phi_e}_0 + \Delta\phi
 \end{aligned}$$



24

Also use the following:

$$\begin{aligned}
 \sin(\theta_e + \Delta\theta) &= \sin \theta_e \underbrace{\cos \Delta\theta}_{\approx 1} + \cos \theta_e \underbrace{\sin \Delta\theta}_{\approx \Delta\theta} \\
 &\approx \sin \theta_e + \Delta\theta \cos \theta_e \\
 \cos(\theta_e + \Delta\theta) &= \cos \theta_e \underbrace{\cos \Delta\theta}_{\approx 1} - \sin \theta_e \underbrace{\sin \Delta\theta}_{\approx \Delta\theta} \\
 &\approx \cos \theta_e - \Delta\theta \sin \theta_e
 \end{aligned}$$



25

We obtain the following linearized equations (taking first order approximations),

$$\begin{aligned}
 X_e + \Delta X - mg(\sin \theta_e + \Delta \theta \cos \theta_e) &= m\Delta \dot{u} \\
 Y_e + \Delta Y + mg\Delta \phi \cos \theta_e &= m(\dot{v} + U_e r) \\
 Z_e + \Delta Z + mg(\cos \theta_e - \Delta \theta \sin \theta_e) &= m(\dot{w} - U_e q) \\
 L_e + \Delta L &= I_{xx}\dot{p} - I_{zx}\dot{r} \\
 M_e + \Delta M &= I_{yy}\dot{q} \\
 N_e + \Delta N &= -I_{zx}\dot{p} + I_{zz}\dot{r} \\
 \Delta \dot{\theta} &= q \\
 \Delta \dot{\phi} &= p + r \tan \theta_e \\
 \Delta \dot{\psi} &= r \sec \theta_e
 \end{aligned}$$



For example

$$X - mg \sin \theta = m(\dot{U} + QW - RV)$$



$$\begin{aligned}
 X &= X_e + \underbrace{\Delta X}_x \\
 \theta &= \theta_e + \Delta\theta \\
 \sin(\theta_e + \Delta\theta) &= \sin\theta_e + \cos\theta_e\Delta\theta \\
 U &= U_e + \underbrace{\Delta U}_u \\
 Q &= \underbrace{Q_e}_0 + \underbrace{\Delta Q}_q \\
 W &= \underbrace{W_e}_0 + \underbrace{\Delta W}_w, \quad qw \text{ negligible} \\
 R &= \underbrace{R_e}_0 + \underbrace{\Delta R}_r \\
 V &= \underbrace{V_e}_0 + \underbrace{\Delta V}_v, \quad rv \text{ negligible}
 \end{aligned}$$



28

$$X_e + \Delta X - mg(\sin\theta_e + \Delta\theta \cos\theta_e) = m\Delta\dot{u}$$

$$X_e - mg \sin\theta_e = 0$$

$$\Delta X - mg \cos\theta_e \Delta\theta = m\Delta\dot{u}$$

$$\Delta X = \begin{bmatrix} X_u & X_w & X_q & X_{\dot{u}} & X_{\dot{w}} & X_{\dot{q}} \end{bmatrix} \cdot \begin{bmatrix} u \\ w \\ q \\ \dot{u} \\ \dot{w} \\ \dot{q} \end{bmatrix} + \Delta X_c$$



29

Longitudinal Equation:

$$\begin{bmatrix} -X_u & -X_w & -X_q & mg \cos \theta_e \\ -Z_u & -Z_w & -(mU_e + Z_q) & mg \sin \theta_e \\ -M_u & -M_w & -M_q & 0 \\ 0 & 0 & 1 & 0 \end{bmatrix} \begin{bmatrix} u \\ w \\ q \\ \theta \end{bmatrix} + \begin{bmatrix} (m - X_{\dot{u}}) & -X_{\dot{w}} & -X_{\dot{q}} & 0 \\ -Z_{\dot{u}} & (m - Z_{\dot{w}}) & -Z_{\dot{q}} & 0 \\ -M_{\dot{u}} & -M_{\dot{w}} & (I_{yy} - M_{\dot{q}}) & 0 \\ 0 & 0 & 0 & -1 \end{bmatrix} \begin{bmatrix} \dot{u} \\ \dot{w} \\ \dot{q} \\ \dot{\theta} \end{bmatrix} = \begin{bmatrix} \Delta X_c \\ \Delta Z_c \\ \Delta M_c \\ 0 \end{bmatrix}$$



30

4. Flight Control Surfaces

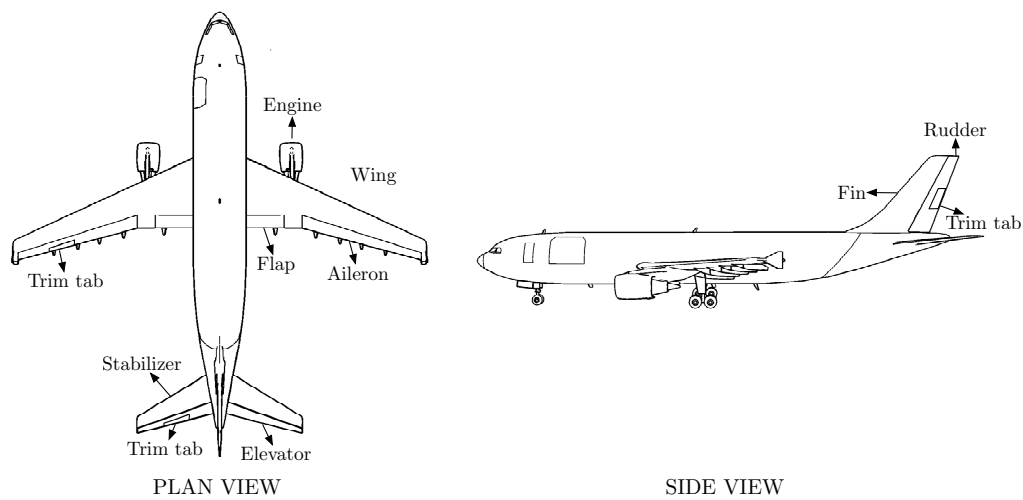


Fig 5: Control surfaces



31

Elevator The column sets the elevator angle to change the pitching moment (nose up or down). It is normally placed at the tail. This surface contribution can be used to put aircraft into climb or dive (throttle must often be adjusted as well). Also it is used to set a new value for angle of attack α to allow level flight at different airspeed (again, throttle change will also be required).



32

Aileron On the outboard (outer one-third or so of the span), the trailing edge on one side of the wing deflects opposite to that on the other. These oppositely moving surfaces are called ailerons. The wheel sets the aileron angle (one up the other down) to cause the aircraft to roll about its longitudinal x -axis. Once the desired bank angle is achieved the aileron are centered leaving the lift vector tilted away from the earth vertical and this causes the aircraft to follow a curved flight path. This the sequence used to turn an aircraft.



33

Rudder The rudder is used to correct for yaw caused by an engine failure or to slip the aircraft using crossed controls (e.g. x -wind landing). Although it is not the primary control for turning, it may be used to correct nose pointing error in a turn.



Linearized Dynamics Diagram

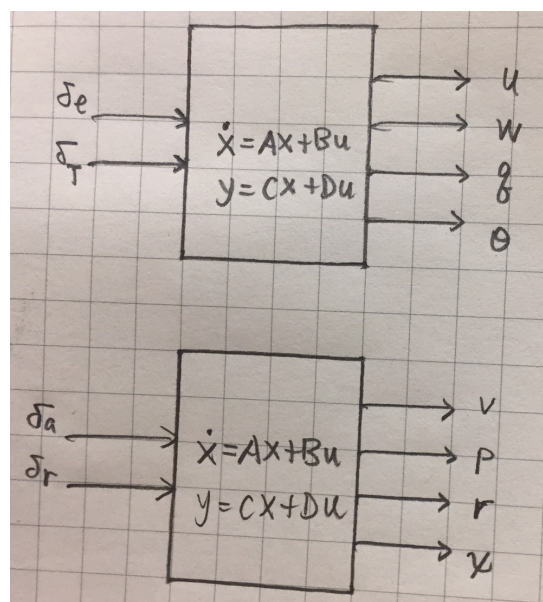


Fig 6: Aerial Vehicle Linearized Dynamics Diagram



5. Mission Profile

to understand what the mission of UAS is, what performance is expected



36

6. Control Design Process

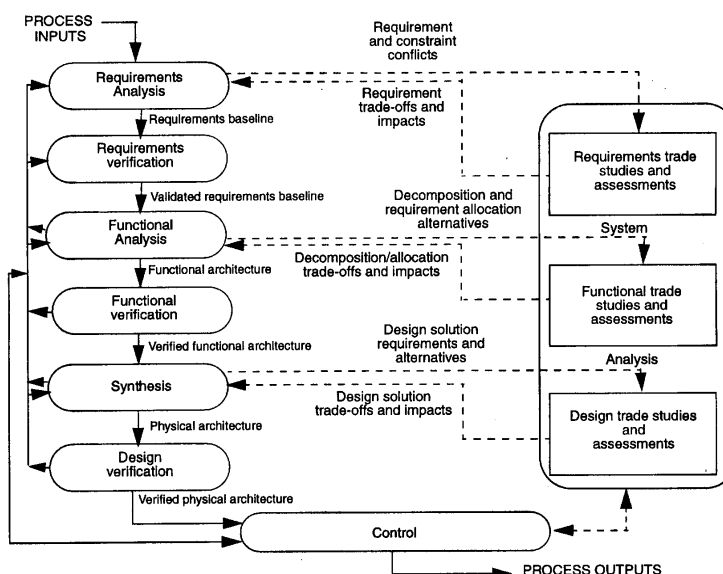


Fig 7: Systems Engineering Process



37

- The requirement analysis is to establish what the system shall be capable of accomplishing. The results are documented in a requirement baseline. At this phase, the designer shall define the expectations, constraints, operational scenarios, interfaces and boundaries, functional and performance requirements. The designer shall also define the technical performance measures (TPMs) as indicators of system performance.
The output is a documented requirements baseline.
- The requirement verification or validation process will be addressed later.
The output is a documented validated requirements baseline.



38

- The functional analysis is to translate the validated requirement baseline (output from the previous requirement validation process) into a functional architecture, without consideration for a design solution.
At this stage, performance requirements are allocated, and failure modes and effects are identified. The output is a functional architecture.
- The functional verification is to assess the completeness of the functional architecture in satisfying the validated requirements baseline and to produce a verified functional architecture.
The output is a verified functional architecture.



39

- Synthesis translates the functional architecture into a design architecture that provides an arrangement of system elements, their decomposition, interfaces, and design constraints.
The output is a design architecture with design characteristics. Design solutions and alternatives are also identified.
- Design verification is performed to ensure that the requirements of the lowest level of the design architecture, are traceable to the verified functional architecture, and the design architecture satisfies the validated requirement baseline.
Low level design requirements also include derived requirements.



40

- Systems analysis is to resolve any identified conflict, evaluate the effectiveness of the design solutions.
The performance improvement and/or optimization is conducted at this stage, including trade-off study, risk handling.



41

System Design Process



42

The aim of system design is to *find* subsystems (components) to represent a solution, given the inputs and desired outputs or tolerable errors, and to integrate them into a functional system that perform its assigned tasks satisfactorily. The design process leading to this end can be broken into several phases that are more or less chronological, yet are extensively interrelated and interconnected.

(1) Establishment of System Purpose and Overall System Requirements. System purpose sometimes is also called mission phase or task definition from the end user (customer). Requirements are partially derived from the operational functions to be performed to accomplish these mission phases, and partially (less directly) derived from the characteristics and the environment (implied requirements).

(2) Determination of Unalterable Element, Command, and Disturbance Environment Characteristics. Examples of “unalterable” elements are: vehicle itself, control surface



43

actuator, structure, etc. Examples of “alterable” elements include sensing and actuating instruments. Control system requirements can be categorized as mission-centered, component-centered, and system-interaction requirements.

(3) Evolution of Competing Feasible Systems. Also at this stage, the basic functional block diagrams are determined. Usually the requirements can be met in more than one way. It is possible to evolve competing candidates for selection on the basis of certain desirable properties.

(4) Competing System Assessment. It is the stage to select system. An optimal system is one that has some “best” combination of all design quantities and qualities. In principle, a complete evolution of functional requirements is the result of an optimization process, and the most fundamental element in this process is the establishment of possible alternative configurations.



(5) Detailed Study of the Selected System. Once a best system has been selected, it is still necessary to validate it for all nominal and abnormal operation conditions, through simulation and testing.

(6) Ground and Flight Testing. The purpose is to ensure that, when the equipment is put into service, it will not have any surprises left for its designers. Another important application of the control test is in the investigation of the results of possible component failures. Final evaluation of the operating characteristics of an automatic flight control system is, of course, made by means of flight tests. Many of the same aircraft input and output quantities that were recorded during the ground tests should be recorded in flight. It is then desirable to explore the conditions that may not have been examined in the ground tests.



Flight Control Systems

- flight control to reduce pilot workload (autopilot)
- landing aid
- stability augmentation
- control augmentation



46

- flight control to reduce pilot workload (autopilot). The slow modes (phugoid and spiral) are controlled by a pilot. It is undesirable for a pilot to have to pay continuous attention to controlling these modes, an automatic control system is needed to provide “pilot relief”. Such a control system is called autopilot.
 - pitch attitude hold
 - altitude hold
 - Bank angle hold
 - turn coordination
 - heading hold
- landing aid
 - glide slope control



47

- localizer to align the aircraft in the lateral direction with the runway centerline
- flare control to make transition from the glide slope to the runway
- stability augmentation, to provide proper stability or ensure appropriate handling qualities
 - roll damper
 - pitch damper
 - yaw damper
- control augmentation to control the mode and to provide the pilot with a particular type of response to the control inputs
 - roll rate
 - pitch rate



48

- normal acceleration



49

Control Specifications

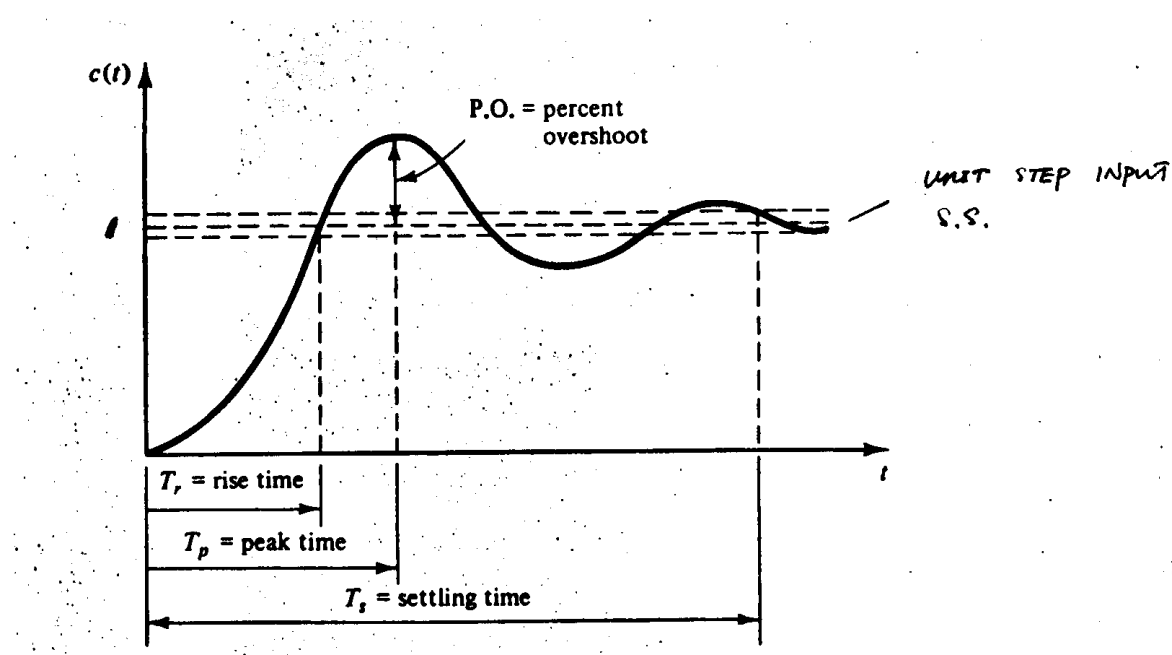


Fig 8: Step Response



50

- **Time Constant T** : the time for the amplitude of oscillation to decay to e^{-1} of its initial value
- **Percentage Overshoot PO** : the maximum percentage overshoot over the steady-state response
- **Peak Time T_p** : the time to the maximum peak of the response
- **Rise Time T_r** : the time at which the response first reaches the steady-state level
- **Settling Time T_s** : the time required for the response to come permanently within a 2% (5%) band of steady-state response



For a pair of complex roots case (second-order system), one has the following conclusion:

$$\text{transfer function} \quad \frac{\omega_n^2}{s^2 + 2\zeta\omega_n s + \omega_n^2} \quad (25)$$

$$\text{unit step response} \quad c(t) = 1 - \frac{1}{\sqrt{1-\zeta^2}} e^{-\zeta\omega_n t}.$$

$$\sin(\omega_n \sqrt{1-\zeta^2} t + \phi) \quad (26)$$

$$\phi = \tan^{-1} \left(\frac{\sqrt{1-\zeta^2}}{\zeta} \right) \quad (27)$$

$$\text{time constant} \quad T = \frac{1}{\zeta\omega_n} \quad (28)$$

$$\text{percentage overshoot} \quad PO = 100 \exp \left(\frac{-\pi\zeta}{\sqrt{1-\zeta^2}} \right) \quad (29)$$

$$\text{peak time} \quad T_p = \frac{\pi}{\omega_n \sqrt{1-\zeta^2}} \quad (30)$$

$$\text{settling time} \quad T_s = 4T = \frac{4}{\zeta}, \quad (31)$$



7. Feedback Control Theory

A typical control system set up

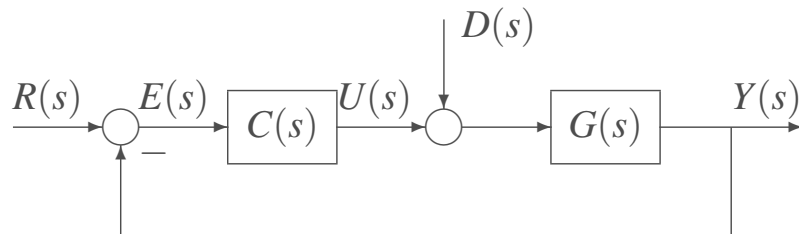


Fig 9: A typical feedback control system

- The open-loop transfer function

$$G_0(s) = C(s)G(s) \quad (32)$$

- The closed-loop transfer function (when $D = 0$)

$$T(s) = \frac{Y(s)}{U(s)} = \frac{C(s)G(s)}{1 + C(s)G(s)} \quad (33)$$



Basic Problems

- **Tracking problem.** Given $G(s)$, find the controller (control system) $H(s)$ to make $E(s)$ small.
- **Disturbance Rejection.** When $R = 0$, we re-draw the previous diagram:

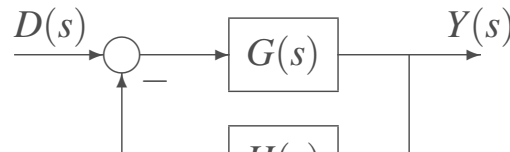


Fig 10: Disturbance rejection

The problem becomes: to keep $y(t)$ small in the presence of disturbance $d(t)$

$$\frac{Y(s)}{D(s)} = \frac{G(s)}{1 + G(s)H(s)}$$

(34) 

54

7.1 Steady-State Error Analysis

Based on the unity gain feedback system

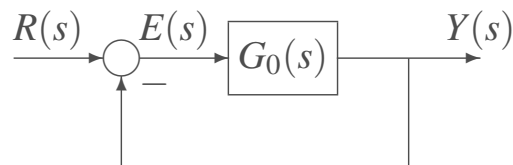


Fig 11: Unity Gain Feedback

The *steady-state error*

$$e_{ss} = \lim_{t \rightarrow \infty} e(t) = \lim_{s \rightarrow 0} sE(s) \quad (35)$$



55

$$E(s) = \frac{1}{1 + G_0(s)} R(s) \quad (36)$$

The **objective**: describe the steady-state error of the closed-loop system based on the open-loop function $G_0(s)$, for the following inputs

- step input, $r(t) = H(t)$
- ramp input, $r(t) = tH(t)$
- parabolic input, $r(t) = \frac{1}{2}t^2H(t)$



The steady-state response $y_{ss}(t)$ of a stable system $G(s)$ to a sinusoidal input $u(t)$ with frequency ω_0 :

$$u(t) = U_0 \sin \omega_0 t$$

is also sinusoidal with the same frequency but it is amplified by $|G(j\omega_0)|$ and has a phase shift $\phi = \arg G(j\omega_0)$:

$$\begin{aligned} y_{ss}(t) &= |G(j\omega_0)| U_0 \sin(\omega_0 t + \phi_0) \\ \phi_0 &= \arg G(j\omega_0) \end{aligned}$$



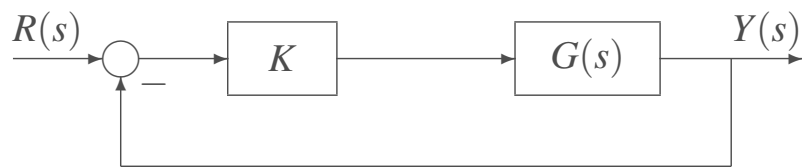
The Bode plots of

- the magnitude $|G(j\omega)|$ ($20 \log_{10} |G(j\omega)|$) vs ω , and
- the phase angle $\arg G(j\omega)$ vs ω



58

Stability Margin



59

Consider the Bode plot of the *open-loop* system $KG(s)$,

- gain crossover frequency ω_g , where $|KG(j\omega)| = 1$, or 0 dB
- phase crossover frequency ω_π , where $\arg KG(j\omega) = -180^\circ$

the stability margins for the *closed-loop* system:

- gain margin, $GM = \left| \frac{1}{KG(j\omega_2)} \right|_{dB}$, $GM > 0$ when $|KG(j\omega_2)|_{dB} < 0dB$
- phase margin, $PM = 180^\circ + \arg KG(j\omega_1)$, $PM > 0$ when $\arg KG(j\omega_1) > -180^\circ$



PID Controllers

- 1 Proportional (P) Control
- 2 Proportional-Derivative (PD) Control
- 3 Proportional-Integral (PI) Control
- 4 Proportional-Integral-Derivative (PID) Control



■ Proportional Control

$$u(t) = K_p e(t) \quad (37)$$

$$U(s) = K_p E(s) \quad (38)$$

■ Proportional-Derivative Control

$$u(t) = K_p e(t) + K_d \dot{e}(t) \quad (39)$$

$$U(s) = (K_p + K_d s) E(s) \quad (40)$$

■ Proportional-Integral Control

$$u(t) = K_p e(t) + K_i \int_0^t e(\tau) d\tau \quad (41)$$

$$U(s) = \left(K_p + \frac{K_i}{s} \right) E(s) \quad (42)$$



■ PID Control

$$u(t) = K_p e(t) + K_i \int_0^t e(\tau) d\tau + K_d \dot{e}(t) \quad (43)$$

$$U(s) = \left(K_p + \frac{K_i}{s} + K_d s \right) E(s) \quad (44)$$



8. Pitch Attitude Control

The characteristic lightly damped, low-frequency oscillation in pitch attitude was identified before, leads to large peaks and long transients. Pitch attitude control is a typical feedback control channel, that the pitch angle is regulated through the control of elevator angle. In this section, we will explore classical design approaches of finding proper controller $C(s)$ as illustrated in Fig.12. Again, we will continue using the [B747-100] case study to illustrate the design concepts and procedure.

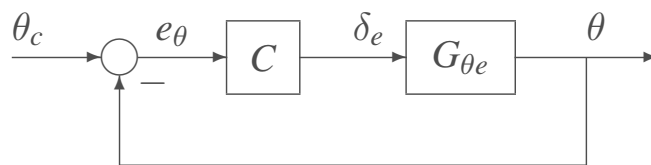


Fig 12: Pitch Attitude Control



First of all, the transfer functions

$$G_{\theta e} = \frac{-1.157s^2 - 0.3537s - 0.003864}{s^4 + 0.7499s^3 + 0.9341s^2 + 0.009449s + 0.004187}$$

where the open-loop zeros and poles are:

$$z_1 = -0.2944, z_2 = -0.0113,$$

$p_{1,2} = -0.0033 \pm 0.0672i, p_{3,4} = -0.3717 \pm 0.8869i$. In the meantime, its phugoid mode approximation

$$G_{\theta e}^{ph} = \frac{-1.412s^2 - 0.428s - 0.004675}{s^2 + 0.009685s + 0.005065}$$

also generating the open-loop zeros and poles:

$$z_1 = -0.2919, z_2 = -0.0113, p_{1,2} = -0.0048 \pm 0.0710i.$$



The following observations are made:

- The step response reveals the long settling time, it implies that the phugoid mode dominates the dynamic behaviour;
- the transfer function has a negative sign, indicating the physics of positive deflection of elevator angle driving negative pitch angle reaction (nose down); it is not a standard transfer function from control design perspective, which is often assumed to be 'positive'. One may use $-G(s)$ for the sake of carrying out design/analysis, to be reminded that a corresponding negative sign of control law will be added to compensate for the actual negative nature of the transfer function.
- Numerically, the steady-state value of θ responding to 1 degree of elevator deflection is settled to be close to -1 degree, $\theta_{ss} = \lim_{t \rightarrow \infty} \theta(t) = \lim_{s \rightarrow 0} s\theta(s) = -0.9$ (deg). The phugoid approximation gives:

$$\theta_{ss} = \frac{c_0}{C} \approx \frac{M_{\delta_e}}{M_w} \frac{X_u}{Z_u} \frac{Z_w}{mg} = -0.82$$
 (deg).



66

To summarize, the typical control specifications are:

- steady state error (tracking accuracy)
- overshoot, or damping ratio, or phase margin (oscillation)



67

Investigate the open-loop frequency response by the Bode plot, again taking the negative $-G_{\theta e}(j\omega)$,

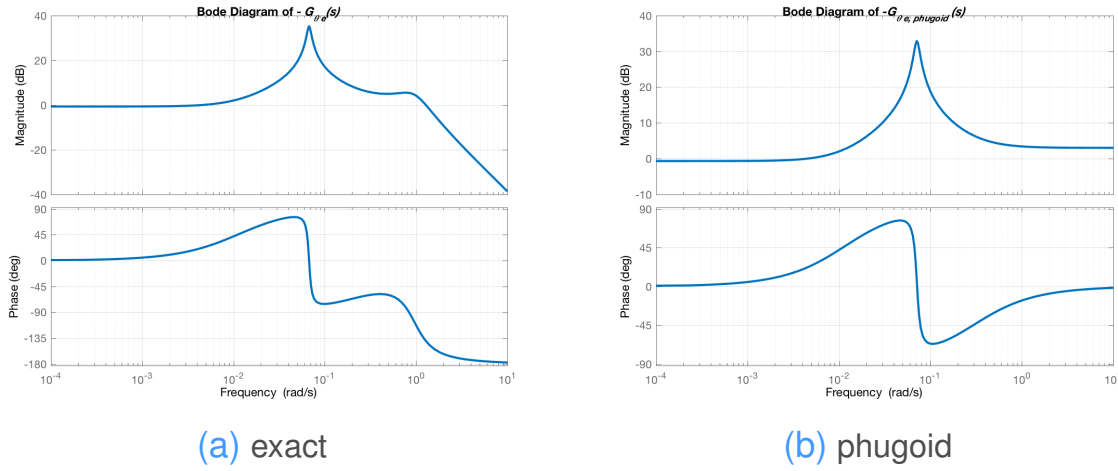


Fig 13: Pitch Control: Frequency Response



showing that the phase margin is at a decent 40 degree, at $\omega_p = 1.2809$ (rad). Unfortunately, if one uses the phugoid approximation only, the Bode plot cannot reveal the high-frequency response, therefore no finite phase margin would be obtained. It suggests that while phugoid mode approximation may be used to replace the exact mode in time-domain analysis, it is better to keep frequency-domain as is.



We may come up with a standard, but relaxed design specifications:

- overshoot less than 25%
- steady state error less than 10%



70

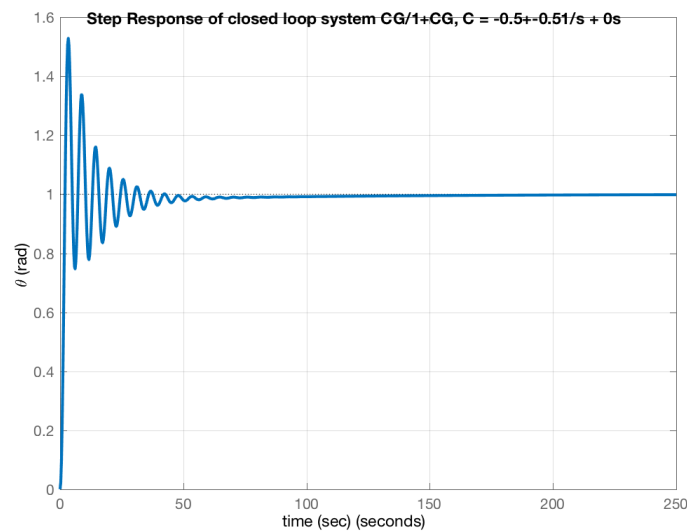


Fig 14: Step Response of Closed-loop System $H = \frac{CG}{1+CG}$,
 $C = K_p + \frac{K_i}{s}$, $K_p = -0.5$, $K_i = -0.5$



71

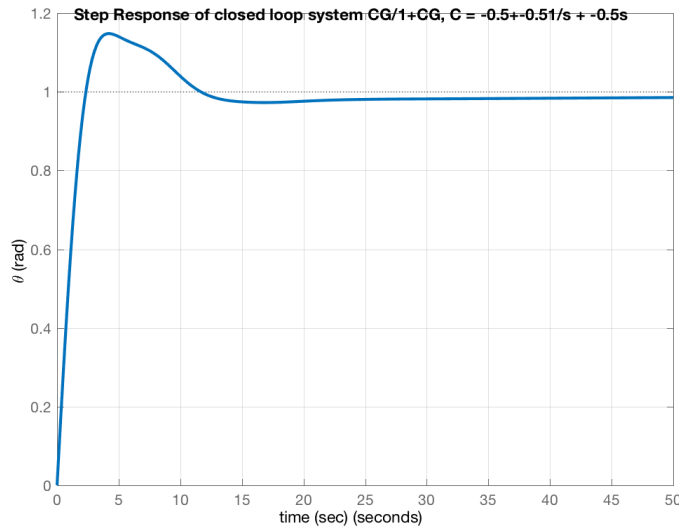


Fig 15: Step Response of Closed-loop System $H = \frac{CG}{1+CG}$,
 $C = K_p + \frac{K_i}{s}, +K_d s, K_p = -0.5, K_i = -0.5, K_d = -0.5$



72

9. Autopilot: Altitude Hold Control

The feedback control channels for individual input and specific state reveals the capability of stabilization and performance regulation through control law design. Essentially, the closed-loop system's dynamic modes are manipulated to provide desired properties. Yet, these control channels alone do not complete the job of offering an operational function in flight. These functions often require coordination of control channels to give the pilot some release of manual control. They are achieved by so-called *autopilot*.



73

One such example of autopilot in the longitudinal flight operation is the *altitude hold control*, where a command altitude is given for the aircraft to maintain at a certain speed. In other words, this autopilot has both altitude and speed control. The overall control structure is illustrated in the following block diagram Fig. ??.



74

Altitude Hold Control

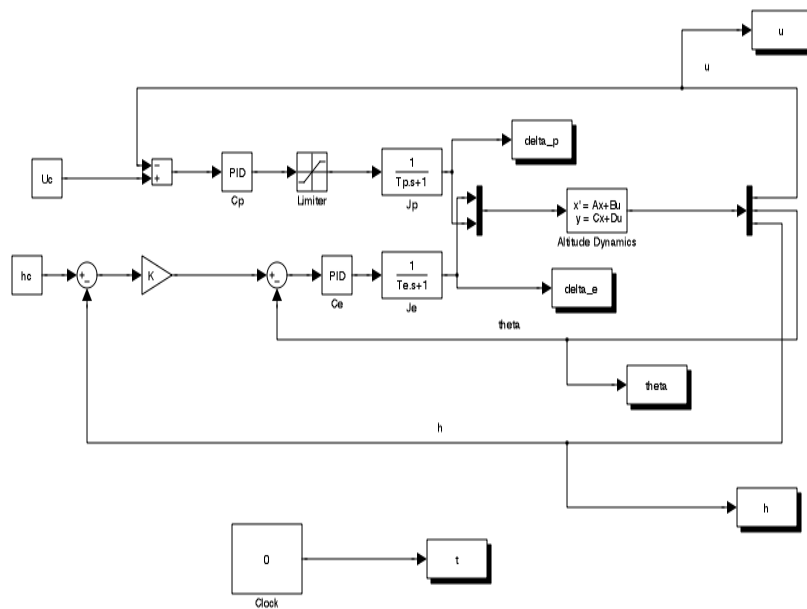


Fig 16: Altitude Hold Control: Block Diagram



75

The altitude control incorporates control of speed, altitude (as well as pitch attitude)

- selection of control channels
- inner/outer loop design structure
- limit of actuation



76

In our [B747-100] case, we set the autopilot function with a new command flight of altitude of 13,000 m with speed of 250 m/s vs the reference point of 12,192 m at 235.9 m/s. If we use the classical approach of PID control, by choosing the following parameters:

$K_{p,u} = 0.015, K_{d,u} = 0.005, K_{p,\theta} = -0.5, K_{i,\theta} = -0.5, K_{d,\theta} = -0.5$, as well as the gain for altitude outer loop $K_h = 0.001$, then we obtain the altitude hold results as follows.



77

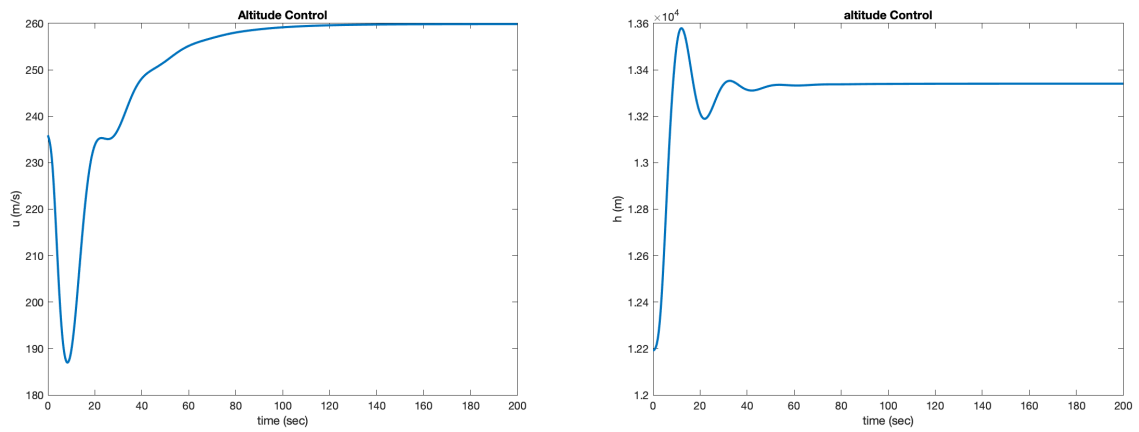


Fig 17: Altitude Hold: PID Simulation



78

10. Procerus Flying Wing System

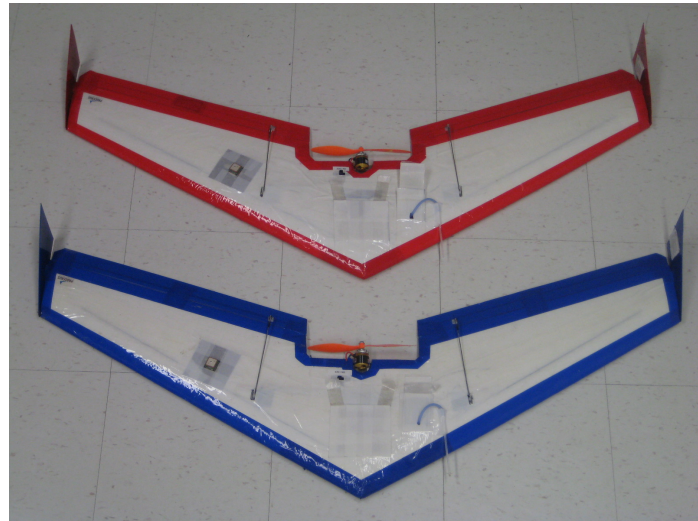


Fig 18: Procerus flying wings



79

10.1 Physical Parameters of Procerus Flying Wing

Wing Data

Span	4 ft
Total Wing Area	2.8 ft^2
Aspect Ratio	5.714
Taper Ratio	0.441
Chord at Tip	0.4 ft
Chord at Root	0.9035 ft
Chord at Tip (including elevon)	0.53 ft
Chord at Root (including elevon)	1.035 ft
Sweep Angle (with respect to LE)	29°
Dihedral Angle	0°
Wing Incidence Angle (uniform)	1°



80

Elevon Data

Chord (uniform)	0.1312 ft
Span (one side)	1.77 ft
Length (one side)	1.8675 ft
Distance from Centerline	0.227 ft
Sweep Angle (same as TE)	17°

Other Parameters

Total Weight	2.2 lb
CG Location (from LE along centerline)	0.6726 ft



10.2 Procerus Kestrel Autopilot I

- The Procerus Kestrel autopilot onboard the UAV is powered by an 8-bit 29 MHz processor.
- It provides autonomous flight control, GPS waypoint navigation as well as autonomous takeoff, flight, and auto-landing routines of unmanned aerial vehicles (UAV).
- It contains a suite of sensors to measure and estimate the states of the aircraft [1].
 - The Kestrel autopilot is also equipped with differential and absolute pressure sensors for sensing the airspeed and barometric altitude of the aircraft.
 - The GPS plugs into the autopilot and provides position, heading, and velocity information necessary for waypoint navigation.



82

10.2 Procerus Kestrel Autopilot II

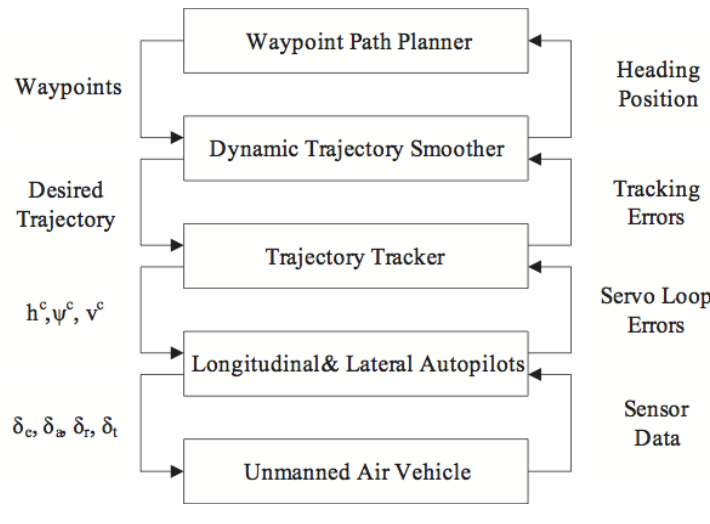
- The Kestrel system combines sensor information with GPS information to provide smooth position and velocity information between GPS samples.
- The autopilot interfaces directly to the digital communication link which enables it to send real-time status telemetry to the ground station and receive commands in-flight through stream of packets. Additional interface ports are available to support payloads.



83

10.3 Control Architecture of Procerus Flying Wing I

The five layers high level system architecture of the Kestrel autopilot is illustrated in Figure 2.2 [2].



84

10.3 Control Architecture of Procerus Flying Wing II

[Fig 19: Autopilot system architecture \[2\]](#)

- The system takes waypoint commands as the primary input and the waypoint path planner generate waypoint paths.
- The trajectory smoother smoothes through these waypoints and produces a feasible reference trajectory.
- The trajectory tracker then outputs the velocity command (v^c), heading command (ψ^c), and altitude command (h^c) to the autopilot based on the desired trajectory.
- The autopilot then uses these commands to control the elevator (δ_e), aileron (δ_a), rudder (δ_r), and throttle (δ_t).



85

10.4 Elevator Control Loop

Figure 20 diagrams the elevator control on the Kestrel autopilot. It is used for longitudinal and airspeed stability of the aircraft. The autopilot determines if the control is driven by altitude or airspeed command, never enabling both at the same time.

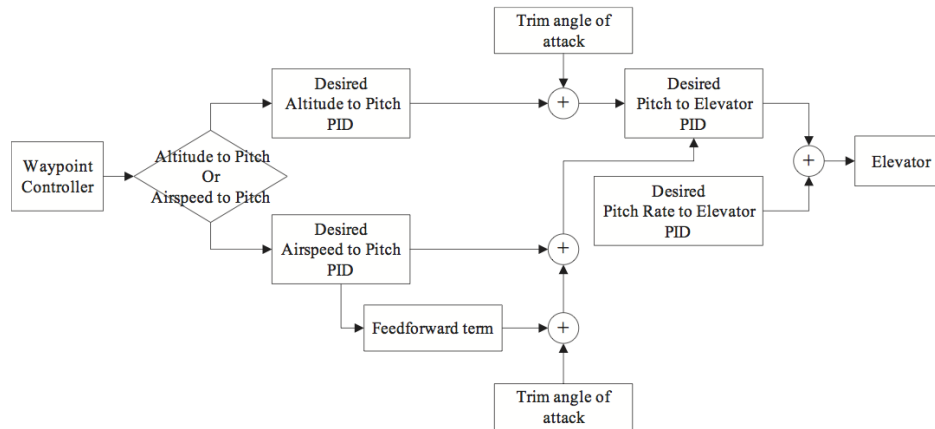


Fig 20: Kestrel autopilot elevator control loop [1]



86

10.5 Throttle Control Loop

The throttle control is used to control airspeed during level flight. Figure 21 shows the diagram for the throttle control. Similarly, the autopilot decides if the throttle is commanded by either altitude or airspeed command, never enabling both at the same time.

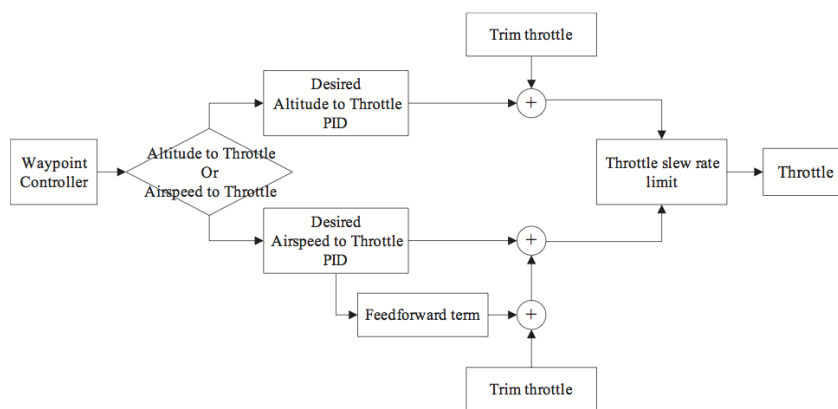


Fig 21: Kestrel autopilot throttle control loop [1]



10.6 Aileron Control Loop

Finally, aileron control is used for lateral stability of the aircraft. Figure 22 diagrams the aileron control on the Kestrel autopilot.

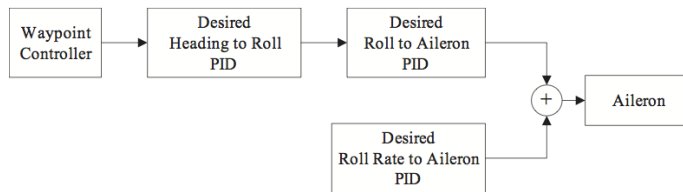


Fig 22: Kestrel autopilot aileron control loop [1]



10.7 Hardware



GumStix, a small form factor miniature computer, is added to each vehicle for controlling the Kestrel autopilot onboard. The formation controller is implemented on the GumStix computer, and the high level trajectory commands to achieve formation are sent to Kestrel autopilot through interfaces.

- The GumStix consist of the verdex XL6P motherboard that provides a Marvell XScale PXA270 processor running at 600MHz with 128MB of SDRAM.
- The Gumstix embedded computer runs a full Linux environment with C/C++ library and a 802.11(b)/802.11(g) wireless expansion board (netwifimicroSD-vx) can be connected to the verdex motherboard through the 120 pin connector to enable wireless capabilities.



90

- The code for the formation controller and drivers for sending commands to the Kestrel autopilot is written in C++ on the GumStix and communication between UAVs are enabled through the wireless expansion board. Figure shows the additional hardware that is to be added to each of the vehicles: the GumStix verdex motherboard and the wireless expansion board.



91

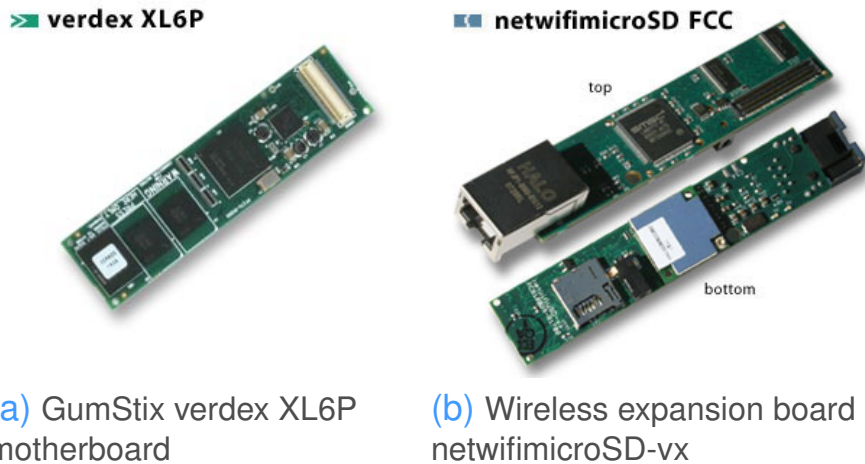


Fig 23: Additional hardware added to control Kestrel autopilot

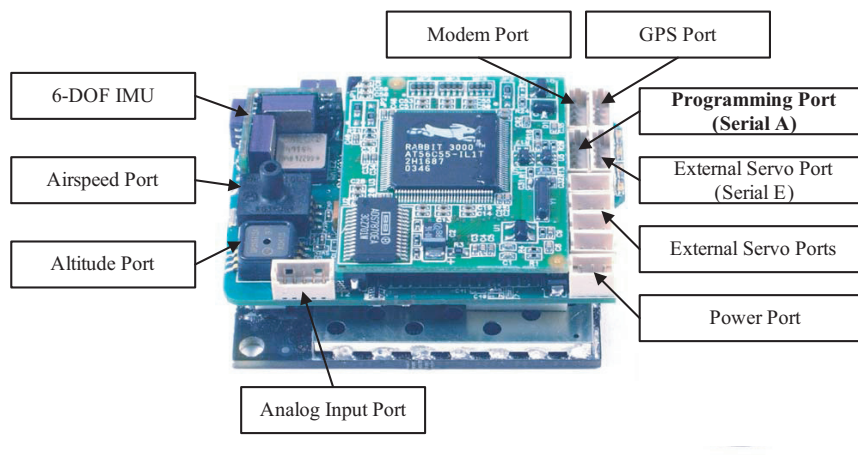


Procerus Kestrel autopilot allows external onboard computer or microcontroller to be connected.

- To integrate the additional processor, serial port A on the autopilot can be configured as a modem port to mirror the actual modem port.
- The autopilot will then accept and reply to commands on the mirror port as if they were sent from the ground station.
- This function can be enabled by configuring the payload settings of the autopilot.
- The serial port can also be configured for standard serial, SPI and I2C communication.



- The following figures show the location and the pin assignments of serial port A on the autopilot respectively. A 5V voltage can be supplied from the serial port to power the addition GumStix board that is to be attached, this can be done by setting the voltage jumper on the back of serial port A.



94

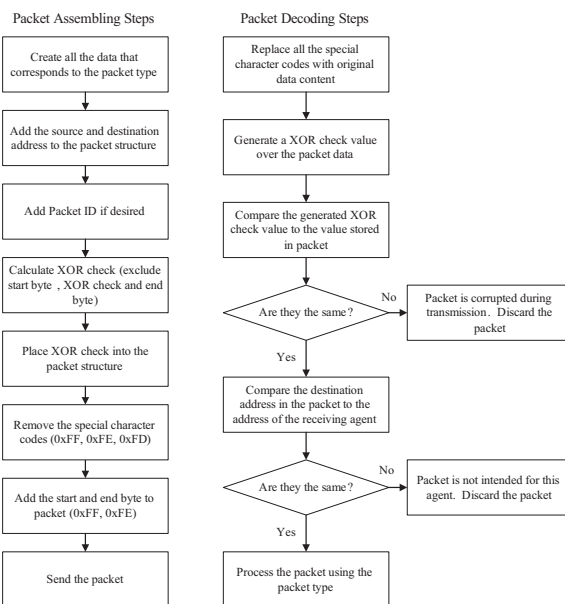
Fig 24: Location of serial port A on Kestrel [1]

10.8 Command and Communication Protocol

Data can be sent between the GumStix and Kestrel using the serial connection depicted in the previous section, but how the autopilot understands commands and what protocol is being used must be understood.



96



It describes the communication schemes between the vehicles and a possible ground station. The ground station may be present for vehicle monitoring purpose, but it is not essential in the formation control experiment as the controller resides on the vehicles' onboard hardware and communication can be enabled between the vehicles natively. Therefore, there are two communication scenarios, where

- the vehicles send information to the ground station, and
- the vehicles communicate between themselves to achieve formation control.



Vehicles to Ground Station Communication

The communication link between the UAVs and the ground station are enabled through the communication device (Commbox) from Procerus Technologies.

- It allows operators to configure, monitor, issue commands and upload flight plans to the autopilots.
- Each autopilot is configured with a unique address so the ground station can identify the source and destination of information flow.
- In the case of the formation project, the device will be used for monitoring the aircraft only. The wireless communication link used is radio frequency operating at 900MHz with an outdoor line of sight range up to 64km. The link will utilize the communication protocol from Procerus.



Vehicle to Vehicle Communication



100

It requires the vehicles to have communication to achieve formation control. This communication link will be established by the additional GumStix hardware with wireless ethernet capability onboard each vehicle through the TCP/IP protocol.

- However, an wireless access point has to be present when working under normal TCP/IP mode to act as a gateway for the communication.
- The disadvantage is all agents must be in the wireless range of the access point in order to successfully establish communication between the agents.
- Since the wireless range using ethernet is approximately in the order of 100 meters, then working with normal TCP/IP mode in the formation project will not be feasible as the UAVs will have the possibility of traveling out of the wireless range of the access point when flying across the test area.



101

- Furthermore, additional delays will be present when data has to be transmitted through an access point to arrive at the destined vehicle.
- The solution to the problem is to enable the ad-hoc network mode for TCP/IP.
- In this network mode, there is no centralized access point required and each mobile agent itself can be considered as an individual access point.
- It is a self-configuring network and the agents in the network are free to move randomly and organize themselves arbitrarily.
- When multiple agents come within the wireless range of each other, a network will be automatically established between them.
- This network scheme is especially suitable for cooperative missions of multiple vehicles due to its capability of connecting agents automatically when they are in range.



102

- The other advantage of the ad-hoc network is the data transmission does not need to go through any centralized gateway except the agents themselves, enabling direct communication between the vehicles and eliminating additional delays.
- This mode can be configured on the GumStix network protocol section, and with the advantages of the communication scheme, it is chosen to be the network setup for vehicle to vehicle communication.



103

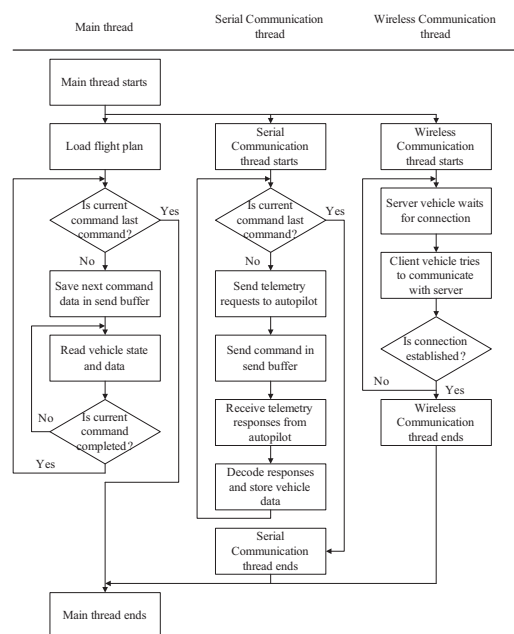
10.9 Flight Controller Implementation

This section describes the software architecture that defines the flight control algorithm to execute UAV flights autonomously with the serial communication to the autopilot and the wireless communication to other vehicles set up. Since the GumStix computer being integrated onto the vehicle has a linux environment with full C/C++ library, the flight control is then developed in C++.

The mission controller is implemented using a multi-threaded architecture. The essential parts of the controller are developed in separate threads for them to execute simultaneously with each other. There are three threads in the program. The overall architecture of the implementation is shown in Figure.



104



105

- ❑ Procerus Technologies, *Kestrel Autopilot System User Guide*, 1.51 ed., August 2007.
- ❑ W. Ren and R. W. Beard, “Trajectory tracking for unmanned air vehicles with velocity and heading rate constraints,” *IEEE Transactions on Control Systems Technology*, vol. 12, pp. 706–716, September 2004.

